



Article

Structural Colored Fabric Based on Monodisperse Cu₂O Microspheres

Xiaowen Li ¹, Zhen Yin ², Zhanghan She ¹, Yan Wang ^{2,3}, Parpiev Khabibulla ⁴, Juramirza Kayumov ⁵ , Guojin Liu ¹, Lan Zhou ¹ and Guocheng Zhu ^{2,3,6,*} 

- ¹ Key Laboratory of Advanced Textile Materials and Manufacturing Technology, Ministry of Education, Zhejiang Sci-Tech University, Hangzhou 310018, China; lxw5201019@163.com (X.L.); 19895921166@163.com (Z.S.); 15757157466@163.com (G.L.); lan_zhou330@163.com (L.Z.)
- ² College of Textile Science and Engineering, Zhejiang Sci-Tech University, Hangzhou 310018, China; 17712107935@163.com (Z.Y.); amywang1021@hotmail.com (Y.W.)
- ³ Zhejiang-Czech Joint Laboratory of Advanced Fiber Materials, Zhejiang Sci-Tech University, Hangzhou 310018, China
- ⁴ Department of Technology of Textile Industry Products, Namangan Institute of Engineering and Technology, 7, Kasansay Street, Namangan 160115, Uzbekistan; parhabib@mail.ru
- ⁵ Department of Civil Engineering, Samarkand State Architecture and Construction University, Samarkand 140143, Uzbekistan; juramirza@gmail.com
- ⁶ Zhejiang Provincial Innovation Center of Advanced Textile Technology, Shaoxing 312000, China
- * Correspondence: gchengzhu@zstu.edu.cn

Abstract: Structural-colored fabrics have been attracting much attention due to their eco-friendliness, dyelessness, and anti-fading properties. Monodisperse microspheres of metal, metal oxide, and semiconductors are promising materials for creating photonic crystals and structural colors owing to their high refractive indices. Herein, Cu₂O microspheres were prepared by a two-step reduction method at room temperature; the size of Cu₂O microspheres was controlled by changing the molar ratio of citrate to Cu²⁺; and the size of Cu₂O microspheres was tuned from 275 nm to 190 nm. The Cu₂O microsphere dispersions were prepared with the monodispersity of Cu₂O microspheres. Furthermore, the effect of the concentration of Cu₂O microsphere and poly(butyl acrylate) on the structural color was also evaluated. Finally, the stability of the structural color against friction and bending was also tested. The results demonstrated that the different structural colors of fabrics were achieved by adjusting the size of the Cu₂O microsphere, and the color fastness of the structural color was improved by using poly(butyl acrylate) as the adhesive.



Citation: Li, X.; Yin, Z.; She, Z.; Wang, Y.; Khabibulla, P.; Kayumov, J.; Liu, G.; Zhou, L.; Zhu, G. Structural Colored Fabric Based on Monodisperse Cu₂O Microspheres. *Materials* **2024**, *17*, 3238. <https://doi.org/10.3390/ma17133238>

Received: 14 May 2024
Revised: 24 June 2024
Accepted: 27 June 2024
Published: 1 July 2024



Copyright: © 2024 by the authors. Licensee MDPI, Basel, Switzerland. This article is an open access article distributed under the terms and conditions of the Creative Commons Attribution (CC BY) license (<https://creativecommons.org/licenses/by/4.0/>).

Keywords: Cu₂O microsphere; photonic crystal; structural color; textile

1. Introduction

Structural color is generated from the interaction of light and microstructures without any role having to be played by dyes or pigments [1,2]. It widely exists in nature, has been researched for a long time, and has attracted much attention due to its advantages of eco-friendliness, brilliant colors, and anti-fading properties [3,4]. The fundamental optical processes of structural color can be defined as thin-film interference, multilayer interference, a diffraction grating effect, light scattering, and photonic crystals [4–8]. Among them, the most commonly applied methods explored are multilayered photonic crystals [9–13] or amorphous photonic structures [14–17] for the structural coloration of textiles.

The widely used colloidal spheres for constructing photonic crystals are polystyrene, polymethyl methacrylate, polysulfide and silica spheres [18–21], which have a relatively low refractive index, resulting in a weak band gap for the photonic crystal and a less brilliant structural color [22]. Some researchers reported that a high refractive index would be helpful for generating brilliant structural color, and metallic microspheres are usually selected [23,24]. Bi [23,24] synthesized Cu₂O microspheres at room temperature for structural

color formation, and distinct colors were obtained on transparent substrates through the structural arrangement of these Cu_2O microspheres. For instance, Han [25] sprayed Cu_2O microspheres of various sizes onto textiles to avoid iridescence and achieve better mechanical stability. Sarwar [26] synthesized cross-linkable nano-cubes of Cu_2O and used them to color and functionalize cotton fabrics simultaneously to obtain self-cleaning, antibacterial fabric based on photocatalytic oxidation reactions. This strategy serves as a potential alternative to toxic chemical dyeing and finishing. The exploration of microspheres of Cu_2O to achieve structural coloration using the spray coating method along with functional properties was extended by Fang [27], in which they finely tuned the size of Cu_2O particles explored the structural color stability and fastness along with their antibacterial properties.

However, there is an essential need to explore the full potential of these photonic crystal structures, i.e., Cu_2O microspheres as building blocks for structural coloration of textiles, the stability of photonic crystals, and the color fastness of structurally colored textiles. Herein, in this research, Cu_2O microspheres in different sizes by a two-step reduction method are proposed and developed, followed by the formulation of Cu_2O microsphere dispersions. The morphology, monodispersity, microstructure, and stability of these Cu_2O microsphere dispersions and the obtained structurally colored fabrics have been assessed in detail. This research would help understand the structurally colored fabrics produced by Cu_2O microspheres in detail and would inspire researchers to develop new technologies.

2. Materials and Methods

2.1. Materials

Copper acetate monohydrate ($\text{C}_4\text{H}_6\text{CuO}_4 \cdot \text{H}_2\text{O}$), sodium citrate dehydrate ($\text{C}_6\text{H}_5\text{Na}_3\text{O}_7 \cdot 2\text{H}_2\text{O}$), polyvinylpyrrolidone (MW = 58,000), ethylene glycol, ascorbic acid, sodium hydroxide, anhydrous ethanol, deionized water (with electrical conductivity 18 $\text{M}\Omega \cdot \text{cm}$) were provided by Shanghai Macklin Biochemical Technology Co., Ltd. (Shanghai, China). The woven polyester fabrics were obtained from Suzhou Feijun Textile Co., Ltd. (Suzhou, China). Poly(butyl acrylate) (MW = 210,000) was purchased from Dayang Chem (Hangzhou) Co., Ltd. (Hangzhou, China). All the chemicals and solvents were analytical grade and were used as received without further purification.

2.2. Preparation of Cu_2O Microsphere

The Cu_2O microspheres were prepared by a two-step reduction method at room temperature. Specifically, 0.32 g of copper acetate monohydrate, 0.52 g sodium citrate, and 1.50 g polyvinylpyrrolidone were dissolved in a mixed solvent of 30 g ethylene glycol and 100 g deionized water to form a homogenous solution under stirring for 20 min at 25 °C. Then, 20 mL of sodium hydroxide solution (0.5 M) was added to the homogenous solution at room temperature with stirring to form a new solution named S1.

A transparent ascorbic acid solution was prepared by dissolving 0.32 g of ascorbic acid in 15 mL of deionized water. A total of 7.5 mL of the ascorbic acid solution was added into solution S1 at a speed of 1 drop per second by using the injection pump. After 5 min, the remaining 7.5 mL of ascorbic acid solution was simultaneously added in the above system under stirring for 60 min to get the solution named S2.

A high-speed centrifuge (TGL-20B-C) from Shanghai Anting Scientific Instrument Factory (Shanghai, China) was used to separate Cu_2O microspheres from solution S2 at a speed of 8000 r/m for 30 min. The as-prepared Cu_2O microspheres were collected and put into an ethanol- H_2O mixture solution, and then the Cu_2O microspheres/ethanol- H_2O solution was separated again in the high-speed centrifuge. After repeating this process three times, the separated Cu_2O microspheres were then dried in a vacuum at 60 °C for 3 h. The different sizes of Cu_2O microspheres were achieved by changing the molar ratio of citrate to Cu^{2+} . The molar ratio of citrate to Cu^{2+} was 0.8, 1, 1.1 and 1.2.

2.3. Preparation of Structural Color Ink

The monodisperse Cu_2O microspheres were added to anhydrous ethanol, and the mixture was stirred for 30 min to obtain a stable ethanol dispersion of the Cu_2O microsphere.

The concentration of Cu₂O microsphere in the mixture dispersion was 0.5%, 1%, 3% and 5%. Then, the poly(butyl acrylate) as the adhesive was added into the mixture dispersion under stirring to form a homogenous solution, i.e., structural color ink. The concentration of poly(butyl acrylate) was 5%, 10%, 15%, 20% and 25%.

2.4. Requirement of Cu₂O Microsphere

The mechanism of structural color produced by photonic crystal follows the Bragg diffraction law in optics, which can be described as Equation (1).

$$m\lambda_{max} = 2d_{hkl} \left(n_{avg}^2 - \sin^2\theta \right)^{1/2} \quad (1)$$

where m is the order of diffraction, λ_{max} is the wavelength corresponding to the maximum peak in the reflected spectral line (i.e., the position of the photonic bandgap), d_{hkl} is the interplanar spacing, n_{avg} is the average refractive index of a three-dimensional array, θ is the angle of incidence of incident light. The interplanar spacing of d_{hkl} can be calculated by Equation (2).

$$d_{hkl} = \frac{\sqrt{2}D}{\sqrt{h^2 + k^2 + l^2}} \quad (2)$$

where D is the average diameter of microspheres, h , k , and l represents the crystal plane index in the crystal structure.

The refractive index of Cu₂O is 2.7 [28], therefore the range of the Cu₂O microsphere's diameter should be between 168 nm and 278 nm for the visible light wavelength range [29]. Additionally, when the monodisperse index (PDI) of the microsphere is less than 0.08 ($PDI \leq 0.08$), the Cu₂O dispersion would have excellent monodispersity, which is helpful for the construction of a photonic crystal [30].

2.5. Characterization Methods

Dynamic Light Scattering and Zeta Potential measurement systems Zetasizer Nano S from Malvern Panalytical (Malvern, UK) was applied to evaluate the size, and the PDI of the Cu₂O microsphere can be obtained according to Equation (3).

$$PDI = \sigma^2 / Z_D^2 \quad (3)$$

where PDI is a monodisperse index, σ is the standard deviation, and Z_D is the hydrated size of the Cu₂O microsphere. The monodispersity of Cu₂O microsphere dispersion is inversely proportional to the PDI.

Specifically, the Cu₂O microsphere dispersion was diluted into transparency, and then the diluted dispersion was put into a quartz cell for testing. The average values were taken from three measurements. The surface morphology of the Cu₂O microsphere was determined using a field emission scanning electron microscope (FESEM, ALTRA55, Carl Zeiss SMT Ltd, Oberkochen, Germany). Fourier transform infrared spectroscopy (FT-IR) analyses were performed to determine the chemical compounds in the obtained Cu₂O microsphere using a Thermo Scientific (Waltham, MA, USA) Nicolet 5700 FT-IR spectrometer with the KBr method. The Cu₂O microsphere and KBr were mixed at a ratio of 1:50, and then the mixture was ground into powder and pressed into a transparent film for testing. The scanning range was 4000–600 cm⁻¹, with a scanning resolution of 4 cm⁻¹ and a scanning frequency of 32 times. X-ray photoelectron spectroscopy XPS, Thermo Scientific K-Alpha (Waltham, MA, USA) was used to determine the element valence of the Cu₂O microsphere, the analysis of the energy spectrum is based on the binding energy of the C1s peak at 284.6 eV. The crystal phase structures of the Cu₂O microsphere were analyzed by an X-ray diffractometer (XRD, K-alpha, Thermo Fisher, Oxford, UK). The dried Cu₂O microspheres were ground into powder as a sample, the emission source was CuK_α ray (wavelength was 0.154178 nm), the scanning speed was 10 °/min, the scanning angle was 10~80°, the electric current and electric voltage were 40 mA and 40 kV, respectively.

2.6. Storage Stability of Cu_2O Microsphere Dispersion

Zeta potential values of Cu_2O microsphere dispersions with different sizes of Cu_2O microsphere were evaluated by a Zeta potential analyzer (Brook-21) from Brookhaven Instruments, Holtsville, NY, USA. The average value was taken from three measurements. The Cu_2O microsphere dispersions were sealed in a polyethylene terephthalate bottle and stored at room temperature (25 °C). After a period of time, the Cu_2O microsphere dispersion was observed to determine whether it was layering by a digital camera. Meanwhile, the diameter and monodispersity of Cu_2O microspheres were analyzed by a dynamic light scattering particle size distribution analyzer to determine their storage stability.

2.7. Characterization of Structural Color and Its Color Fastness

The structural color generated by Cu_2O microsphere photonic crystal was observed by a 3D video microscope (KH-7700 from QUESTAR China Limited, Shanghai, China). The refractivity of structural color was evaluated by UV-VIS spectrophotometer Lambda-35 by PerkinElmer (Waltham, MA, USA), and the observation angle was perpendicular to the sample (90°).

The bending test: the abatement of structural color and the abscission of photonic crystal were observed before and after the bending test. Specifically, the structural colored fabric with a size of 6 cm × 6 cm was folded in the middle until the two ends were contacted, and then the structural colored fabric was opened. The process was repeated 150 times, and then the fabric was evaluated. The friction test: the rubbing fastness test was carried out by referring to the standard ISO 105-X12:2016 (Textiles—Tests for color fastness Part X12: Color fastness to rubbing) [31]. Specifically, the structural colored fabric was placed and fixed on a flat plane, and then a weight of 50 g was put onto the fabric, the weight was moved on the surface of fabric from one side to another side. The process was repeated for 150 times, and then the fabric was evaluated.

3. Results and Discussion

3.1. Morphology of Cu_2O Microsphere

The Cu_2O microspheres have smooth surfaces, excellent sphericity, and uniform size. Cu_2O microspheres with four different sizes were synthesized under different conditions, which were 275 nm, 240 nm, 210 nm, and 190 nm, respectively (Figure 1).

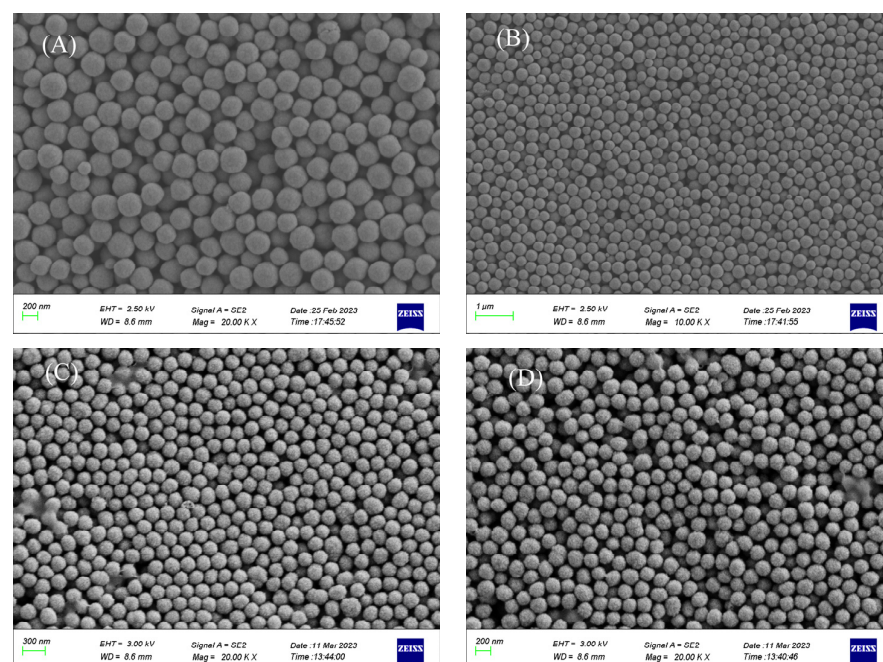


Figure 1. Morphology of Cu_2O microsphere with different sizes (A) 275 nm (B) 240 nm (C) 210 nm (D) 190 nm.

3.2. Analysis of Monodispersity of Cu_2O Microsphere

The diameter and monodispersity of the Cu_2O microsphere were tuned by changing the molar ratio of citrate to Cu^{2+} . It was found that the diameter of the Cu_2O microsphere had a positive correlation with the molar ratio of citrate to Cu^{2+} , i.e., the increase in molar ratio led to an increase in Cu_2O microsphere diameter (Figure 2). The Cu_2O microsphere had monodispersed indices of less than 0.08 (Figure 2), which indicated that the synthesized Cu_2O microspheres have excellent stability and monodispersity [30]. Therefore, the synthesized Cu_2O microspheres would have a suitable dispersion for the construction of photonic crystals.

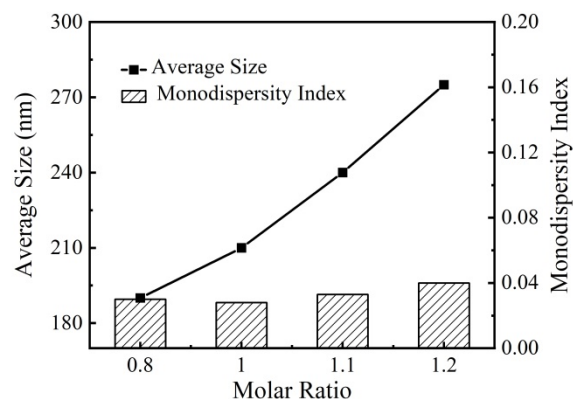


Figure 2. The effect of the molar ratio of citrate to Cu^{2+} on the diameter and monodispersity of the Cu_2O microsphere.

3.3. Microstructure of Cu_2O Microsphere

The structural composition of Cu_2O microspheres was analyzed by FTIR. C=O stretching vibration absorption peak was observed at 1632 cm^{-1} , this peak is wider than the carbonyl absorption peak of polyvinylpyrrolidone (PVP), which is due to the overlapping of the carboxyl asymmetric stretching vibration peak (1598 cm^{-1}) and the carbonyl absorption peak of citrate [32]. The symmetric contraction vibration absorption peak of carboxylic acid in Cu_2O microspheres was found at 1415 cm^{-1} , and the stretching vibration peak of Cu-O was found at 630 cm^{-1} ; refer to Figure 3. The FTIR analysis indicated that there were PVP and carboxylate ions on the Cu_2O microsphere.

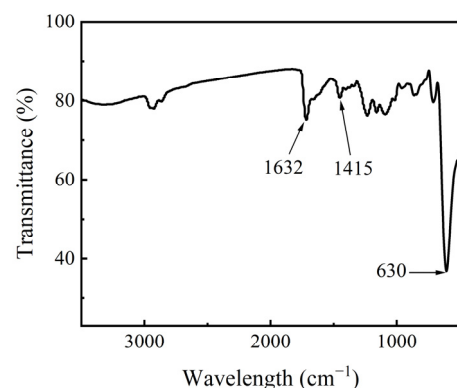


Figure 3. FTIR of Cu_2O microsphere with a diameter of 275 nm.

In order to further understand the purity and composition of the Cu_2O microsphere, XPS testing was carried out. The Cu 2p spectrum shows a sharp main peak at 932 eV (Figure 4A), which corresponds to Cu^{2+} in Cu_2O . At 934 eV, there is a very weak peak corresponding to Cu^{2+} in CuO. The appearance of Cu^{2+} in the product is due to the oxidation of the surface part of the microsphere.

The O 1s spectrum of Cu₂O microspheres also shows two peaks: the peak at 531 eV belongs to O in Cu₂O (Figure 4B), and the small peak at 530 eV belongs to O in CuO. The appearance of Cu²⁺ in the product is due to the oxidation of the surface part of the microsphere. Although the XPS spectrum confirms the presence of CuO in the product, the content of CuO is relatively small, which may only be due to the oxidation of the surface of the microsphere.

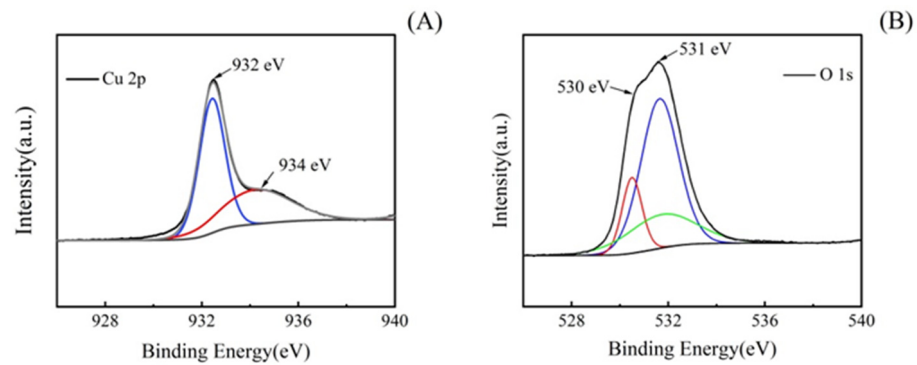


Figure 4. XPS spectrum of Cu₂O microsphere with a diameter of 275 nm. **(A)** The Cu 2p spectrum of the Cu₂O microsphere. **(B)** The O 1s spectrum of the Cu₂O microsphere

3.4. XRD of Cu₂O Microsphere

In order to determine the purity and crystal structure of Cu₂O microspheres, XRD tests were conducted on the prepared Cu₂O microspheres. As shown in Figure 5, the Cu₂O microspheres are consistent with the standard spectrum of cubic Cu₂O in PDF No. 05-0667 refer to Figure 5B. From Figure 5A, it can also be seen that there are no impurity peaks in the product, indicating that the Cu₂O microsphere has a relatively pure crystal phase.

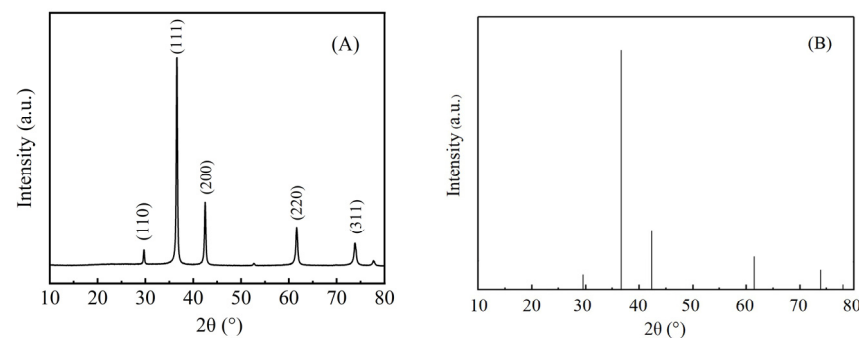


Figure 5. XRD spectrum of **(A)** Cu₂O microsphere with a diameter of 275 nm, **(B)** Cu₂O (PDF#05-0667).

3.5. Zeta Potential Analysis of Cu₂O Microsphere Dispersion

The stability of the Cu₂O microsphere dispersion can be evaluated by observing the absolute value of the Zeta potential difference between the continuous phase of the particles and the liquid stable layer. Usually, when the absolute value of the Zeta potential of particles in the aqueous phase is greater than or equal to 30 mV, it is considered that the dispersion stability of the system is good [33].

The Zeta potential values of Cu₂O microsphere dispersions were −31.24 mV, −32.34 mV, −30.85 mV, and −33.43 mV, corresponding to the diameters of Cu₂O microsphere 275 nm, 240 nm, 210 nm, and 190 nm (the data are given in Table 1). All the absolute Zeta potential values were over 30 mV, indicating that the microspheres are not easy to agglomerate, and the dispersions had good dispersion.

Table 1. Diameter of Cu₂O microsphere and Zeta potential value.

Sample	Diameter of Cu ₂ O Microsphere (nm)	Zeta Potential (mV)
Cu ₂ O microsphere dispersions	275	−31.24
	240	−32.34
	210	−30.85
	190	−33.43

As shown in Figure 6A, as the storage time increased, the particle size of the microspheres showed a stable trend, which indicated that the size of the microspheres exhibited excellent uniformity. However, the monodispersity index PDI of the microsphere dispersions showed a fluctuation trend when the storage time increased, as shown in Figure 6B. But the PDI of all dispersions after storage still did not exceed 0.08, which further proved that the Cu₂O microspheres had good monodispersity. Therefore, the Cu₂O microsphere dispersions synthesized in this study meet the requirements for constructing photonic crystal structures.

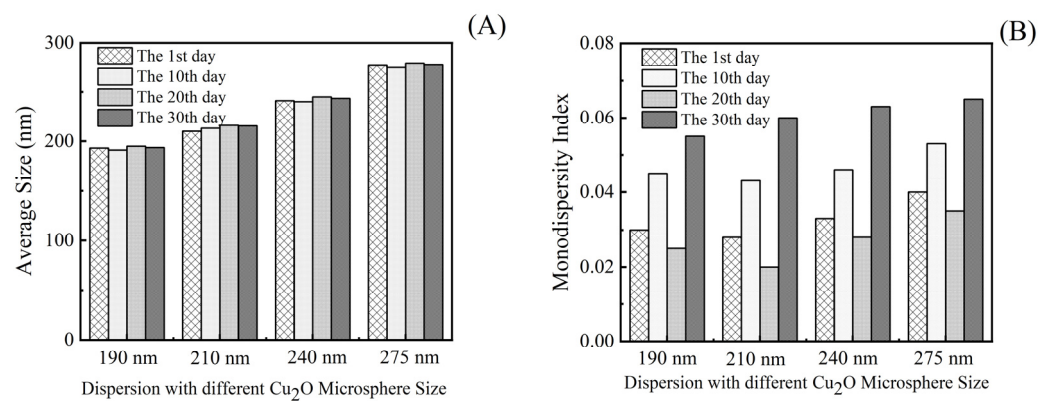


Figure 6. The effect of storage time on (A) the diameter of the Cu₂O microsphere, (B) the monodispersity of the Cu₂O microsphere.

3.6. Effect of Concentration of Cu₂O Microsphere on Structural Color

The Cu₂O microspheres obtained by centrifugation were dry particles that were prone to aggregate together and could not be directly applied to the spray preparation of structural color patterns. In order to solve this problem, the Cu₂O microsphere was added to anhydrous ethanol with different concentrations from 0.5 wt.% to 5.0 wt.%. The Cu₂O microspheres with a size of 240 nm were successfully applied to fabrics, which demonstrated structural colors; refer to Figure 7. The structural colors changed obviously when the concentration of Cu₂O microsphere increased from 0.5 wt.% to 5.0 wt.%. When the concentrations of Cu₂O microsphere were 0.5 wt.% and 1.0 wt.%, though the fabric showed a structural color effect, most of the fabric's background color could still be observed. Moreover, the structural color effect on the fabric was brighter when the mass fraction of microspheres increased to 3.0 wt.%, while the texture of the fabric can also be seen; refer to Figure 7C. Furthermore, when the mass fraction of microspheres was 5.0 wt.%, the fabric surface became fully covered. Although the structural color can be seen on the fabric, the structural layer became thicker, and the structural color began to turn whiter, as shown in Figure 7D.

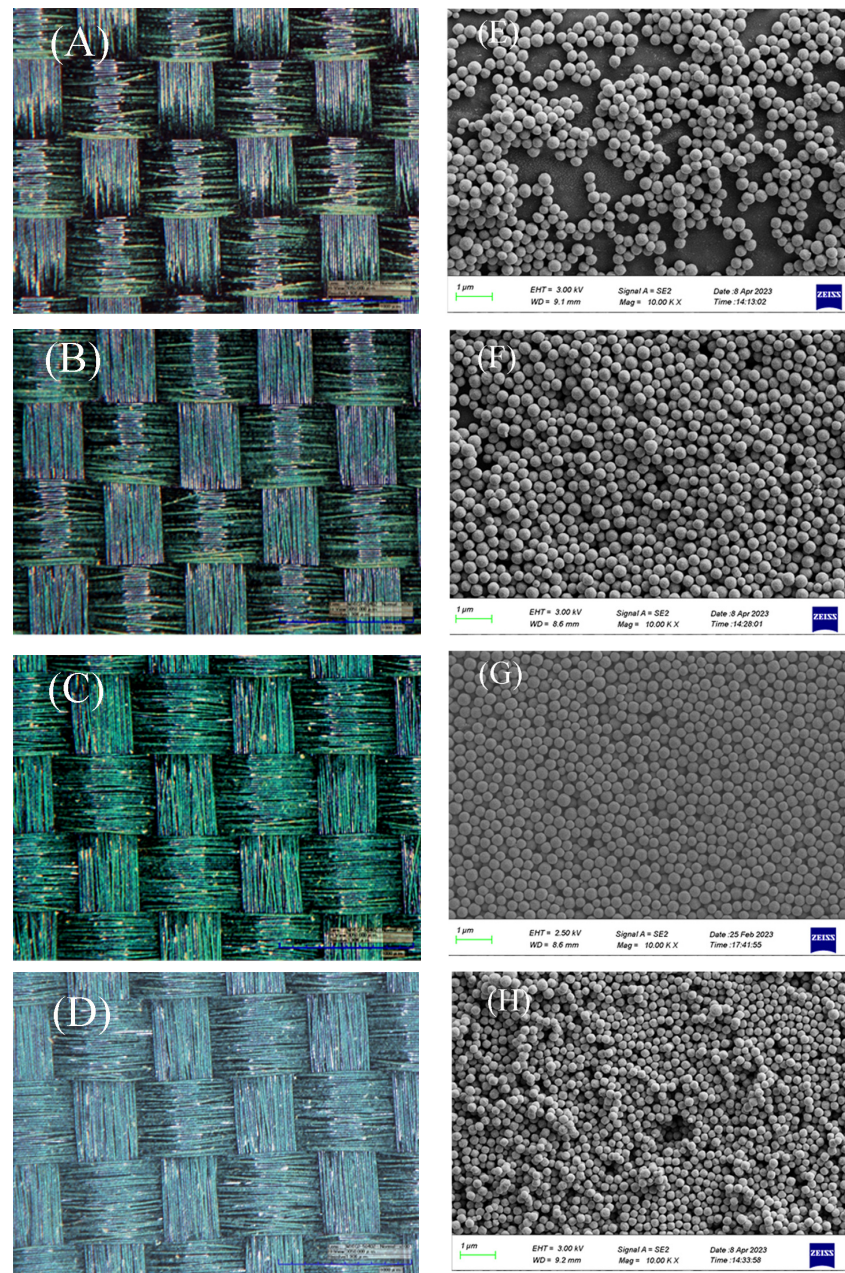


Figure 7. The structural color of fabrics with different Cu₂O microsphere concentration (A) 0.5 wt.%; (B) 1.0 wt.%; (C) 3.0 wt.%; (D) 5.0 wt.%; (E–H) the SEM images of Cu₂O microspheres.

The arrangement of Cu₂O microspheres was observed as well and given in Figure 7E–H. The concentration of Cu₂O microspheres had an effect on their arrangement. When the concentration of the Cu₂O microsphere was 0.5 wt.%, the Cu₂O microsphere was partially regularly arranged, and there were many gaps among the Cu₂O microsphere (Figure 7E), which led to a structural color with low brightness. Meanwhile, the Cu₂O microsphere was not well covered with the fabrics, leading to the appearance of fabric (Figure 7A). When the mass fraction was 1.0 wt.%, the concentration of microspheres was still low and the arrangement was irregular (Figure 7F), which had a certain impact on the arrangement of the photonic crystal structure and on the structural color. When the mass fraction of microspheres reached 3.0 wt.%, the arrangement of microspheres became dense and orderly (Figure 7G), thus presenting a bright and brilliant structural color. When the mass fraction of microspheres reached 5.0 wt.%, the arrangement of microspheres was relatively irregular and overlaid (Figure 7H), resulting in a poor structural color effect on the fabric.

It is worth noting that when the concentration of microspheres in the structural color ink was too low, gaps were generated during the assembly process due to the lower number of microspheres, which ultimately affected the tightness of the arrangement of the microspheres. As the mass fraction of microspheres gradually increased, the arrangement of microspheres became regular and uniform. However, when the concentration of Cu_2O microspheres was too high, a large number of microspheres would collide with each other, thus affecting the formation of the regular self-assembly structure. Based on the above analysis, when the mass fraction of microspheres was 3.0 wt.%, it is possible to establish a photonic crystal chromogenic structure with good integrity and structural color effect on the textile substrate.

3.7. Effect of Concentration of Adhesive on Structural Color

Generally, colloidal microsphere structural primitives have brighter structural colors after self-assembly; however, their bonding fastness with the substrate is often poor, which limits their practical application. To improve its mechanical strength, an adhesive is generally added to the system. Although the fastness is improved after the adhesive is added, the structural color effect becomes worse, or a redshift occurs.

The effect of different poly(butyl acrylate) ratios on structural color patterns was investigated by observing the surface morphology and color of fabrics. It can be seen that when the adhesive ratio was between 5.0 wt.% and 10.0 wt.%, the surface of the fabric was completely covered by the photonic crystal structural color, and the fabric texture can be seen, showing a bright structural color (Figure 8A,B). When the ratio of poly(butyl acrylate) exceeded 10.0 wt.%, although the fabric surface also showed structural color, it started to appear slightly whitened (Figure 8C,D). When the ratio of poly(butyl acrylate) was 25.0 wt.%, the photonic crystal structural color almost changed (Figure 8E). The results had the agreement with other research work that the adhesive will change the performance of structural color [34].

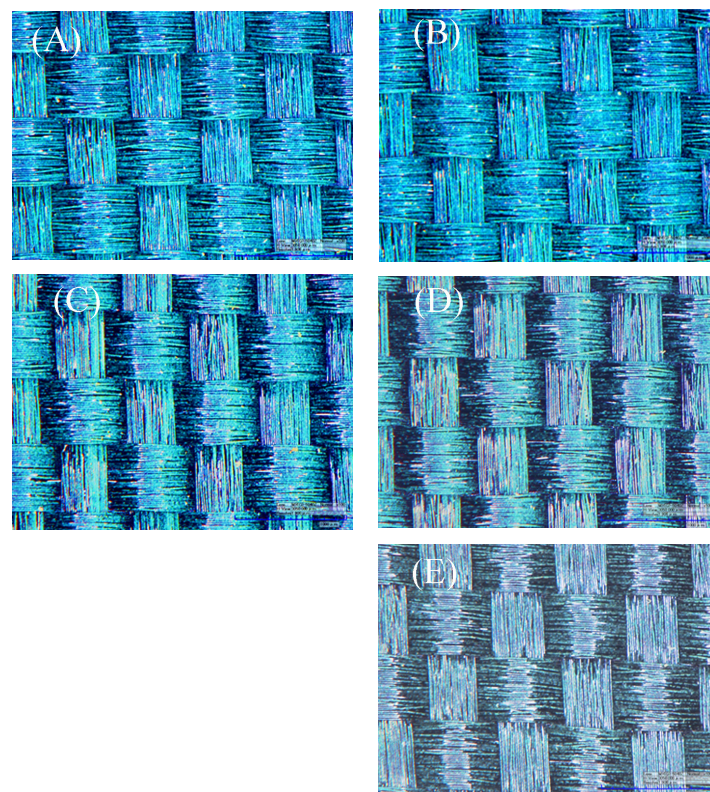


Figure 8. The effect of concentration of poly(butyl acrylate) on structural color. (A) 5.0 wt.%; (B) 10.0 wt.%; (C) 15.0 wt.%; (D) 20.0 wt.%; (E) 25.0 wt.%.

3.8. Effect of Size of Cu_2O Microsphere on Structural Color

Using the spraying method, Cu_2O microsphere structural color ink with different particle sizes was used to construct a structural color pattern on the surface of the textile substrate. The results are given in Figure 9. It can be seen that the structural color pattern integrity and structural color effect constructed were good, and the structural color was tuned by changing the size of Cu_2O microsphere. When the size of Cu_2O microsphere increased, the spacing among the Cu_2O microsphere increased as well, which led to a shifting of the reflected wavelengths to longer wavelengths, i.e., to a redder color [35].

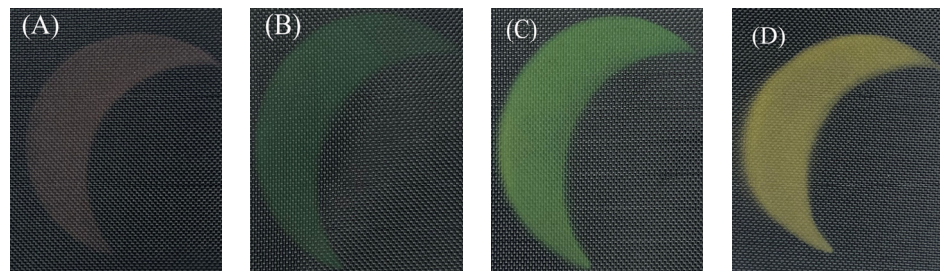


Figure 9. Structural color from Cu_2O microsphere with different sizes (A) 190 nm (B) 210 nm (C) 240 nm (D) 275 nm.

The reflectivity of the constructed structural color patterns was evaluated, and the results are presented in Figure 10. The structural color pattern formed by microspheres of various particle sizes showed a high level of reflectivity and a sharp reflection peak, which means that the structural color effect was good. Meanwhile, the reflection spectra of the structure colors also had a similar trend with the photographs, i.e., the larger size of the Cu_2O microsphere tended to be a redder color.

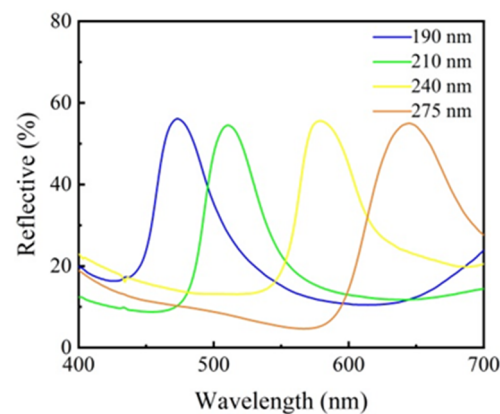


Figure 10. Reflectance curves of structural colored fabrics by adding 5.0 wt.% poly(butyl acrylate) to Cu_2O microspheres with different particle sizes, i.e., 275 nm, 240 nm, 210 nm, and 190 nm.

3.9. Stability of Photonic Crystal

3.9.1. Bending Test

The structural colored fabric for the bending test was prepared by using Cu_2O microspheres with a diameter of 240 nm; the concentration of Cu_2O microspheres was 3.0 wt.%, and the concentration of poly(butyl acrylate) was 5.0 wt.%. After the bending test, the structurally colored fabrics still demonstrated the same bright color (Figure 11(A1–A4)). The structures of the Cu_2O photonic crystal before and after the bending test were also observed by SEM, which showed that the Cu_2O photonic crystal was orderly arranged and did not have a detachment phenomenon after the bending test (Figure 11(B1,B2)). This could be due to the bonding function of poly(butyl acrylate), which provided a solid interface strength and stable structural color.

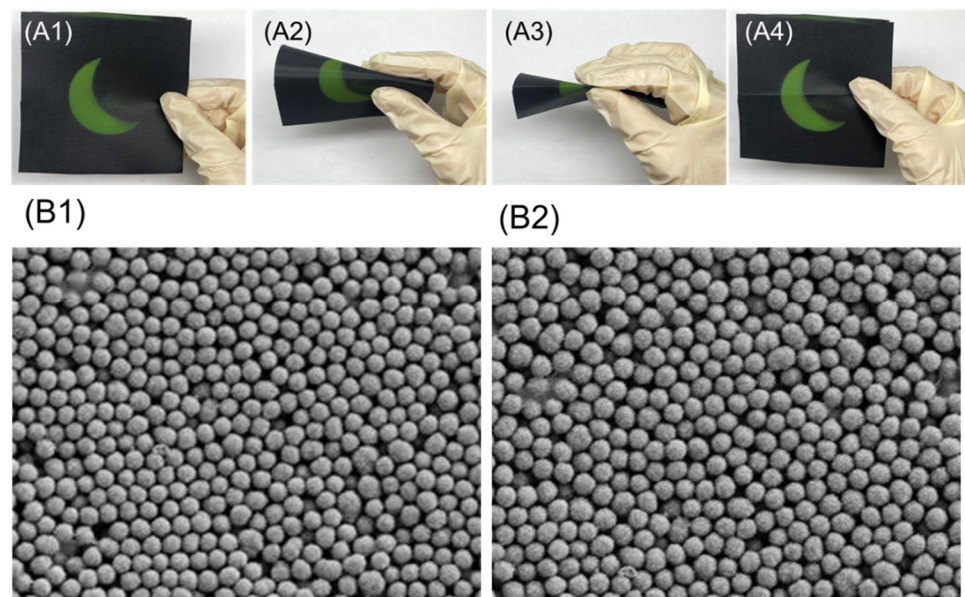


Figure 11. Bending test of structural colored fabric, (A1–A4) Bending test process. (B1) SEM image of photonic crystal before bending test; (B2) SEM image of photonic crystal after bending test.

3.9.2. Friction Test

The structural colored fabric was prepared by using Cu_2O microspheres with a diameter of 210 nm; the concentration of Cu_2O microspheres was 3.0 wt.%, and the concentration of poly(butyl acrylate) was 5.0 wt.%. A friction test was conducted to evaluate the stability of the structural color pattern. The results demonstrated that the structural color was the same color before and after the friction test (Figure 12(A1–A4)), which indicated that the Cu_2O photonic crystal had a stable structure. The SEM images of Cu_2O photonic crystal before and after the friction test showed that there was almost no difference in the arrangement of Cu_2O microspheres and no shedding of Cu_2O observed (Figure 12(B1,B2)). The results also approved that the poly(butyl acrylate) as adhesive improved the stability of photonic crystals and the color fastness of structurally colored fabrics, indicating excellent durability of structural color.

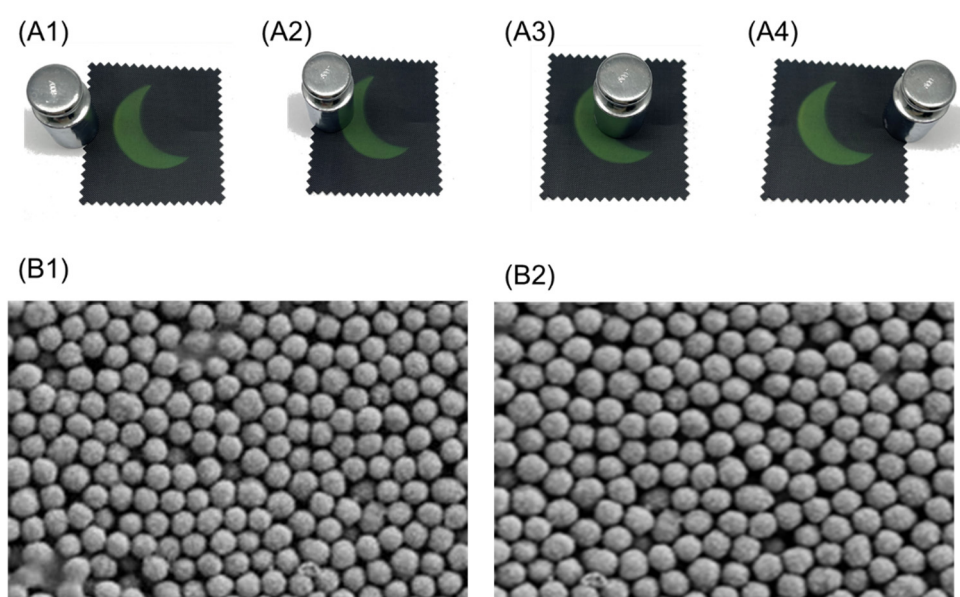


Figure 12. Friction test of structural colored fabric, (A1–A4) friction test process; (B1) SEM image of photonic crystal before friction test; (B2) SEM image of photonic crystal after friction test.

4. Conclusions

Cu₂O microspheres in different sizes and monodisperse indices have been achieved by controlled synthesis for structural color textiles. The surface morphology, monodispersity, microstructure, and stability of Cu₂O microsphere dispersions were rigorously assessed. The effect of the molar ratio of citrate to Cu²⁺ on size and monodispersity and the microstructure of Cu₂O microspheres were also studied in detail. The important parameters, including the composition, purity, and crystal structure to assure the quality of the microspheres of the synthesized Cu₂O microspheres, were confirmed by FTIR, XPS, and XRD. The effect of the concentration of Cu₂O microsphere and adhesive on the structural color performance was also assessed. The adhesive strength of the Cu₂O microspheres and fabric was increased by adding poly(butyl acrylate) as an adhesive. The microspheres were well bound enough so that they could resist frictional and bending forces. This study would be useful to advance and fine-tune the structural coloration of fabrics with better mechanical stability.

Author Contributions: Methodology, G.L.; validation and the reproducibility of experiments, Z.Y. and J.K.; investigation, X.L.; writing—original draft preparation, Z.S.; writing—review and editing, Y.W.; supervision and leadership responsibility for the research activity planning and execution, P.K. and L.Z.; funding acquisition and research activity planning and execution, G.Z. All authors have read and agreed to the published version of the manuscript.

Funding: The work was supported by the Key Program for International S&T Innovation Cooperation Projects of China (Project No.: 2022YFE0125900).

Institutional Review Board Statement: Not applicable.

Informed Consent Statement: Not applicable.

Data Availability Statement: Data is contained within the article.

Conflicts of Interest: The authors declare no conflict of interest.

References

1. Shawkey, M.D.; D'Alba, L. Interactions between color-producing mechanisms and their effects on the integumentary colour palette. *Philos. Trans. B* **2017**, *372*, 1–9. [[CrossRef](#)]
2. Zhu, K.; Fang, C.; Pu, M.; Song, J.; Wang, D.; Zhou, X. Recent advances in photonic crystal with unique structural colors: A review. *J. Mater. Sci. Technol.* **2023**, *141*, 78–99. [[CrossRef](#)]
3. Cuthill, I.C.; Allen, W.L.; Arbuckle, K.; Caspers, B.; Chaplin, G.; Hauber, M.E.; Hill, G.E.; Jablonski, N.G.; Jiggins, C.D.; Kelber, A.; et al. The Biology of Color. *Science* **2017**, *357*, eaan0221. [[CrossRef](#)]
4. Kinoshita, S.; Yoshioka, S. Structural Colors in Nature: The Role of Regularity and Irregularity in the Structure. *ChemPhysChem* **2005**, *6*, 1442–1459. [[CrossRef](#)]
5. Kinoshita, S.; Yoshioka, S.; Miyazaki, J. Physics of structural colors. *Rep. Prog. Phys.* **2008**, *71*, 076401. [[CrossRef](#)]
6. Parker, A.R. 515 million years of structural colour. *J. Opt. A Pure Appl. Opt.* **2000**, *2*, R15–R28. [[CrossRef](#)]
7. Yoshioka, S.; Shimizu, Y.; Kinoshita, S.; Matsuhana, B. Structural color of a lycaenid butterfly: Analysis of an aperiodic multilayer structure. *Bioinspir. Biomim.* **2013**, *8*, 045001. [[CrossRef](#)]
8. Teyssier, J.; Saenko, S.V.; van der Marel, D.; Milinkovitch, M.C. Photonic crystals cause active colour change in chameleons. *Nat. Commun.* **2015**, *6*, 6368. [[CrossRef](#)]
9. Meng, Y.; Tang, B.; Ju, B.; Wu, S.; Zhang, S. Multiple Colors Output on Voile through 3D Colloidal Crystals with Robust Mechanical Properties. *ACS Appl. Mater. Interfaces* **2017**, *9*, 3024–3029. [[CrossRef](#)]
10. Wang, X.; Li, Y.; Zhao, Q.; Liu, G.; Chai, L.; Zhou, L.; Fan, Q.; Shao, J. High Structural Stability of Photonic Crystals on Textile Substrates, Prepared via a Surface-Supported Curing Strategy. *ACS Appl. Mater. Interfaces* **2021**, *13*, 19221–19229. [[CrossRef](#)]
11. Zhou, L.; Li, Y.; Liu, G.; Fan, Q.; Shao, J. Study on the correlations between the structural colors of photonic crystals and the base colors of textile fabric substrates. *Dye. Pigment.* **2016**, *133*, 435–444. [[CrossRef](#)]
12. Liu, G.; Zhou, L.; Zhang, G.; Li, Y.; Chai, L.; Fan, Q.; Shao, J. Fabrication of patterned photonic crystals with brilliant structural colors on fabric substrates using ink-jet printing technology. *Mater. Des.* **2017**, *114*, 10–17. [[CrossRef](#)]
13. Khan, M.R.; Kim, H.G.; Park, J.S.; Shin, J.W.; Nguyen, C.T.; Lee, H.B.R. Tunable Color Coating of E-Textiles by Atomic Layer Deposition of Multilayer TiO₂/Al₂O₃ Films. *Langmuir* **2020**, *36*, 2794–2801. [[CrossRef](#)]
14. Zhou, C.; Qi, Y.; Zhang, S.; Niu, W.; Ma, W.; Wu, S.; Tang, B. Rapid fabrication of vivid noniridescent structural colors on fabrics with robust structural stability by screen printing. *Dye. Pigment.* **2020**, *176*, 108226. [[CrossRef](#)]

15. Li, Y.; Chai, L.; Wang, X.; Zhou, L.; Fan, Q.; Shao, J. Facile Fabrication of Amorphous Photonic Structures with Non-Iridescent and Highly-Stable Structural Color on Textile Substrates. *Materials* **2018**, *11*, 2500. [[CrossRef](#)]
16. Shi, X.; He, J.; Wu, L.; Chen, S.; Lu, X. Rapid fabrication of robust and bright colloidal amorphous arrays on textiles. *J. Coat. Technol. Res.* **2020**, *17*, 1033–1042. [[CrossRef](#)]
17. Zeng, Q.; Ding, C.; Li, Q.; Yuan, W.; Peng, Y.; Hu, J.; Zhang, K.-Q. Rapid fabrication of robust, washable, self-healing superhydrophobic fabrics with non-iridescent structural color by facile spray coating. *RSC Adv.* **2017**, *7*, 8443–8452. [[CrossRef](#)]
18. von Freymann, G.; Kitaev, V.; Lotsch, B.V.; Ozin, G.A. Bottom-up assembly of photonic. *Chem. Soc. Rev.* **2013**, *42*, 2528–2554. [[CrossRef](#)]
19. Galisteo-López, J.F.; Ibisate, M.; Sapienza, R.; Froufe-Pérez, L.S.; Blanco, Á.; López, C. Self-assembled photonic structures. *Adv. Mater.* **2011**, *23*, 30–69. [[CrossRef](#)]
20. Ma, W.; Xiang, J.; Zhang, J.; Li, Y.; Luan, Y.; Zhao, Y.; Chai, L.; Zhu, G.; Zhou, L.; Shao, J.; et al. Preparation and formation mechanism of colorful photonic crystals on rough yarns. *Prog. Org. Coatings* **2024**, *186*, 108029. [[CrossRef](#)]
21. Liu, G.; Han, P.; Wu, Y.; Li, H.; Zhou, L. The preparation of monodisperse P(St-BA-MAA)@disperse dye microspheres and fabrication of patterned photonic crystals with brilliant structural colors on white substrates. *Opt. Mater.* **2019**, *98*, 109503. [[CrossRef](#)]
22. Han, M.G.; Shin, C.G.; Jeon, S.J.; Shim, H.; Heo, C.J.; Jin, H.; Kim, J.W.; Lee, S. Full Color Tunable Photonic Crystal from Crystalline Colloidal Arrays with an Engineered Photonic Stop-Band. *Adv. Mater.* **2012**, *24*, 6438–6444. [[CrossRef](#)]
23. Bi, J.; Wu, S.; Xia, H.; Li, L.; Zhang, S. Synthesis of monodisperse single-crystal Cu₂O spheres and their application in generating structural colors. *J. Mater. Chem. C* **2019**, *7*, 4551–4558. [[CrossRef](#)]
24. Bi, J.; Wu, Y.; Li, L.; Zhang, S.; Wu, S. Asymmetric structural colors based on monodisperse single-crystal Cu₂O spheres. *Nanoscale* **2019**, *12*, 3220–3226. [[CrossRef](#)]
25. Han, Y.; Meng, Z.; Wu, Y.; Zhang, S.; Wu, S. Structural Colored Fabrics with Brilliant Colors, Low Angle Dependence, and High Color Fastness Based on the Mie Scattering of CuO Spheres. *ACS Appl. Mater. Interfaces* **2021**, *13*, 57796–57802. [[CrossRef](#)]
26. Sarwar, N.; Kumar, M.; Humayoun, U.B.; Dastgeer, G.; Nawaz, A.; Yoon, D. Nano coloration and functionalization of cellulose drive through in-situ synthesis of cross-linkable Cu₂O nano-cubes: A green synthesis route for sustainable clothing system. *Mater. Sci. Eng. B* **2023**, *289*, 116284. [[CrossRef](#)]
27. Fang, Y.; Chen, L.; Zhang, Y.; Chen, Y.; Liu, X. Construction of Cu₂O single crystal nanospheres coating with brilliant structural color and excellent antibacterial properties. *Opt. Mater.* **2023**, *138*, 113724. [[CrossRef](#)]
28. Gong, L.; Qiu, Y.; Nan, F.; Hao, Z.; Zhou, L.; Wang, Q. Synthesis and Largely Enhanced Nonlinear Refraction of Au@Cu₂O Core-Shell Nanorods. *Wuhan Univ. J. Nat. Sci.* **2018**, *23*, 418–423. [[CrossRef](#)]
29. Bartolucci, S.F.; Leff, A.C.; Maurer, J.A. Gold-copper oxide core-shell plasmonic nanoparticles: The effect of pH on shell stability and mechanistic insights into shell formation. *Nanoscale Adv.* **2024**, *6*, 2499–2507. [[CrossRef](#)] [[PubMed](#)]
30. Liu, G.; Zhou, L.; Wu, Y.; Wang, C.; Fan, Q.; Shao, J. Optical properties of three-dimensional P(St-MAA) photonic crystals on polyester fabrics. *Opt. Mater.* **2015**, *42*, 72–79. [[CrossRef](#)]
31. *ISO 105-X12:2016*; Textiles—Tests for Colour Fastness Part X12: Colour Fastness to Rubbing. International Organization for Standardization: Geneva, Switzerland, 2016.
32. Kyzioł, A.; Łukasiewicz, S.; Sebastian, V.; Kuśtrowski, P.; Kozieł, M.; Majda, D.; Cierniak, A. Towards plant-mediated chemistry—Au nanoparticles obtained using aqueous extract of *Rosa damascena* and their biological activity in vitro. *J. Inorg. Biochem.* **2020**, *214*, 111300. [[CrossRef](#)] [[PubMed](#)]
33. Montes, C.; Villaseñor, M.J.; Ríos, A. Analytical control of nanodelivery lipid-based systems for encapsulation of nutraceuticals: Achievements and challenges. *Trends Food Sci. Technol.* **2019**, *90*, 47–62. [[CrossRef](#)]
34. Li, Y.; Zhou, L.; Liu, G.; Chai, L.; Fan, Q.; Shao, J. Study on the fabrication of composite photonic crystals with high structural stability by co-sedimentation self-assembly on fabric substrates. *Appl. Surf. Sci.* **2018**, *444*, 145–153. [[CrossRef](#)]
35. Ge, J.; Yin, Y. Responsive Photonic Crystals. *Angew. Chem. Int. Ed.* **2011**, *50*, 1492–1522. [[CrossRef](#)] [[PubMed](#)]

Disclaimer/Publisher’s Note: The statements, opinions and data contained in all publications are solely those of the individual author(s) and contributor(s) and not of MDPI and/or the editor(s). MDPI and/or the editor(s) disclaim responsibility for any injury to people or property resulting from any ideas, methods, instructions or products referred to in the content.